

Cellular Decomposition for Non-repetitive Coverage Task with Minimum Discontinuities

Tong Yang¹, Jaime Valls Miro² *Member, IEEE*, Qianen Lai¹, Yue Wang^{1*} and Rong Xiong¹

Abstract—A mechanism to derive non-repetitive coverage path solutions with a proven minimal number of discontinuities is proposed in this work, with the aim to avoid unnecessary, costly end effector lift-offs for manipulators. The problem is motivated by the automatic polishing of an object. Due to the non-bijective mapping between the workspace and the joint-space, a continuous coverage path in the workspace may easily be truncated in the joint-space, incurring undesirable end effector lift-offs. Inversely, there may be multiple configuration choices to cover the same point of a coverage path through the solution of the Inverse Kinematics. The solution departs from the conventional local optimisation of the coverage path shape in task space, or choosing appropriate but possibly disconnected configurations, to instead explicitly explore the least number of discontinuous motions through the analysis of the structure of valid configurations in joint-space. The two novel contributions of this paper include proof that the least number of path discontinuities is predicated on the surrounding environment, independent from the choice of the actual coverage path; thus has a minimum. And an efficient finite cellular decomposition method to optimally divide the workspace into the minimum number of cells, each traversable without discontinuities by any arbitrary coverage path within. Extensive simulation examples and real-world results on a 5 DoF manipulator are presented to prove the validity of the proposed strategy in realistic settings.

Index Terms—Cellular Decomposition, Non-repetitive Coverage Task, Non-redundant Manipulator

I. INTRODUCTION

THE non-repetitive *coverage task* of a given object is an important application carried out by manipulators. This is for instance the case of inspecting a surface for defects at close range [1], painting [2], deburring [3] or polishing [4]. The task is effectively encapsulated as the generic coverage path planning (CPP) [5] [6] problem, which requires for the end-effector (EE) to traverse over all the points that define the surface of a given object exactly one time, whilst usually fulfilling additional task-specific constraints (e.g. sustaining a desired orientation of the EE with respect to the surface, maintain contact or exerting a constant EE force/torque). This is in contrast to error reduction-driven motion planning schemes for robotic tasks requiring high precision, such as repetitive motion planning (RMP) [7], or so-called cycling motion generation (CMG) schemes [8], notably attractive for repetitive automated industrial production processes.

¹ Tong Yang, Qianen Lai, Yue Wang and Rong Xiong are with the State Key Laboratory of Industrial Control and Technology, Zhejiang University, P.R. China.

² Jaime Valls Miro is with the Centre for Autonomous Systems (CAS), University of Technology Sydney (UTS), Sydney, Australia.

* Corresponding Author.

E-mail address: wangyue@iipc.zju.edu.cn

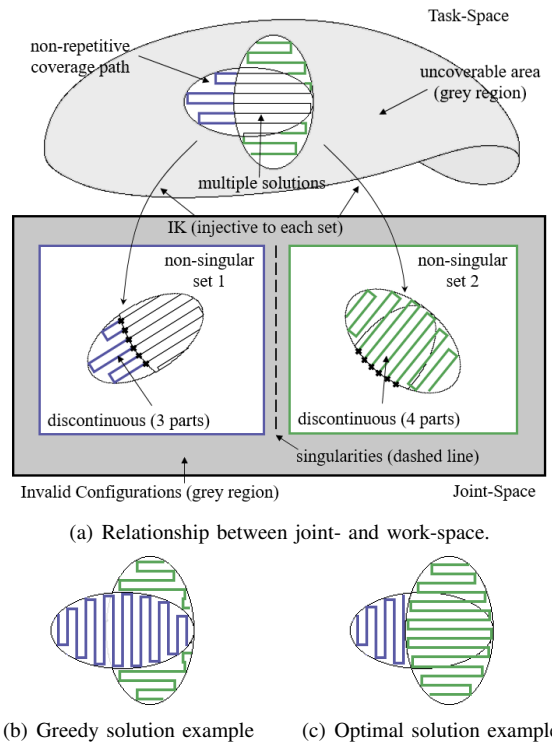


Fig. 1. (a) Illustration of the coverage task problem and the relationship between joint- and work-space. Different colours denote disjoint sets of non-singular joint configurations (arbitrarily, blue may for instance represent those with elbow-up, whilst green may represent elbow-down), and their corresponding path shown in black have unique IK solutions. However, multiple IK solutions exist for the intersecting area shown in black. The underlying continuous coverage path sought out thus becomes intermittent in the workspace after mapping onto the joint-space. In this example, whatever choice among the multiple IK solutions, six discontinuities are required (depicted by black crosses), since the path has three separate segments in set 1, and four in set 2. The case where the joint-space solutions are taken in full from set 2 (green) is depicted. (b) Starting from a configuration belonging to set 1, without explicitly calculating the reachable boundary of each set, the boundary of the set 2 within the reachable area of set 1 is unknown. So a greedy strategy will fully cover the set 1, dividing the uncovered region into two parts, leading to an extra lift-off. On the other hand, although at first sight it may appear the same as using the greedy strategy starting from set 2. (c) illustrates the concept of CPP optimality in the joint space, whereby the continuity of the reachable area is explicitly considered, thus producing a coverage path with a single EE lift-off.

Typically, joint-space dimension is higher than the workspace's, and the Inverse Kinematic (IK) mapping between task and joint space is thus non-bijective. As a result, planning in the higher dimension joint-space cannot ensure non-repetitive visiting, and coverage paths are thus more suited to be designed directly in the workspace domain [9].

Yet what constitutes a continuous coverage path in the

workspace may easily end up truncated into many seemingly *intermittent* sections after mapping them back onto the joint-space, with undesirable path discontinuities, as graphically illustrated by Fig. 1. This is also the case if a simplistic greedy strategy is followed, as the example depicted in Fig. 1(b), whereby a complete path in task space that solves for all possible configurations leads to unnecessary lift-offs to accomplish full coverage.

Singularities have been proven to be at the origin of these bifurcations of the joint-space [10] [11], sitting at the intersection of different configurations (e.g. elbow-up and elbow-down). Notwithstanding singularities, for non-redundant manipulators, non-singular configurations thus form disjoint sets in the joint-space, as illustrated in Fig. 1, and continuous joint-space paths between sets must then visit singularities along the way for full coverage. The problem is further compounded by additional task constraints, most notably obstacles, which produce usable configurations further divided into many disjoint sets, inevitably incurring undesirable “jumps” between sets for successful coverage, as very rarely the whole workspace ends up mapped into a single set.

This work advocates for the minimisation of the cost incurred on these path discontinuities, which can significantly outweigh any improvements proposed in the literature that may occur locally in the task space when it comes to coverage [12]. This is perhaps more apparent for the case of the uniform polishing task motivating this work, as that means lifting the EE off the object’s surface, adjusting the pose of the manipulator to the new configuration, and landing back into contact with the surface again. This may be not only sub-optimal for the speedy completion of the CPP task, but also introduces potentially avoidable complexity in transitioning between position and force/torque control [13] [14] [15] during the coverage task.

In this work, a mechanism is proposed to address this shortcoming and derive CPP solutions with a proven minimal number of discontinuities, with the aim to avoid unnecessary, costly EE lift-offs. The solution departs from locally optimising the shape of the coverage path in task space, or choosing appropriate but possibly disconnected configurations, but explicitly seeking for least number of discontinuous motions through a novel cellular decomposition analysis of the structure of valid configurations in the joint-space. A conceptual illustration is given in Fig. 2. The two novel contributions of this paper can be summarised as:

- 1) Proving that the minimum number of path discontinuities, or “lift-offs”, for the non-repetitive coverage task with non-redundant manipulators is independent of the actual choice of coverage path. Instead, it is predicated on the surrounding environment - the relative pose between manipulator, object and the presence of any obstacles - and this motivates to formulate the problem as a global cellular decomposition process. On a side note, this also implies that the proposed scheme can be exploited as a criterion to evaluate the most advantageous placement of a manipulator, or object to be manipulated (e.g. polished, painted), both in a fixed

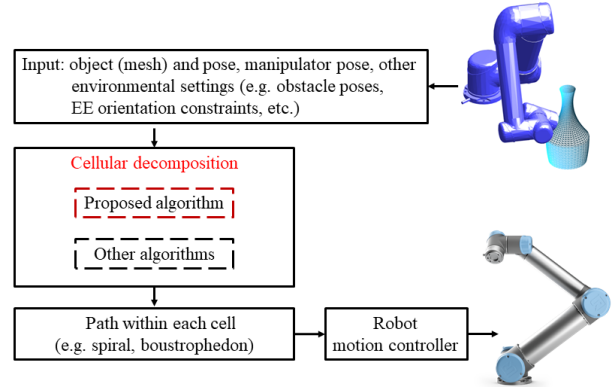


Fig. 2. The role of the novel algorithm for the coverage task. The proposed instrument is compatible with any other existing cellular decomposition solutions whilst also eliciting a minimum number of path discontinuities due to pose reconfigurability.

configuration (automated production line), or in a mobile manipulation environment.

- 2) Proposing an effective finite cellular decomposition method to divide a workspace surface into the least number of cells whereby each is ensured to be traversable by any arbitrary inner path without incurring discontinuities.

The remainder of this paper¹ is organised as follows. Section II reviews existing literature. Section III describes the proposed abstraction of the problem into a topological graph of surface cells corresponding to feasible, continuous configurations, hence administering the tools to prove that the number of path discontinuities for the CPP problem can be made independently to the eventual coverage path chosen. Section IV goes into further details about the process of finitely resolving the surface into cell elements, whilst Section V reports on the proposed iterative strategy to build on the cell elements to ensure CPP with a minimum number of discontinuities. Experimental results from simulations and on an actual non-redundant manipulator are collected in Section VI, with final concluding remarks gathered in Section VII.

II. RELATED WORK

Almost all state-of-the-art methods to solve the CPP problem first divide the robot’s workspace area and then solve the CPP problem in each cell, so called cellular decomposition, which is generally further divided into two categories: exact cellular decomposition methods [16] and Morse-based cellular decomposition methods [17] [18]. Exact cellular decomposition methods divide the free space into several simple, easy sub-regions, and use conventional coverage paths, such as trapezoidal [19] or the boustrophedon paths [20] [21], to finish coverage in each cell. Morse-based cellular decomposition methods apply divisions of the free space based on the critical points of Morse functions to present more flexible shapes for cells over those extracted by exact cellular decomposition. A combination of Morse decomposition and Voronoi

¹A video illustrating the concepts and results hereby described can be found here: <https://www.youtube.com/watch?v=gvXin60cCQ&feature=youtu.be>

diagrams [22] has also been proposed, particularly fitting to cover vast open spaces and narrow areas simultaneously.

Optimality of CPP algorithms mainly focus on metrics such as path length and time to completion. Atkar *et al.* [23] optimised the coverage path through choosing optimal starting points. Huang [24] reduced movement cost by remaining on straight paths as long as possible thus minimising the number of turns. Jimenez *et al.* [25] used a genetic algorithm to achieve optimal coverage. Whilst generic, the context of these coverage works has almost invariably been motivated by mobile robots operating on 2- or 2.5-dimensional terrains. However, for manipulator, this essay advocates avoiding unnecessary path lift-off discontinuities as that decidedly outweighs any other performance metric improvement that may be achieved during the coverage process, e.g. by switching between differing geometric paths such as boustrophedon and spirals as proposed in the works of Hassan and Liu [12]. These discontinuities in the CPP task are inherent to the kinematics of manipulator mechanisms, and as such the algorithms designed for mobile robots do not need to deal with this problem. We notice that [26] considered the pose optimisation of a mobile manipulator for coverage, searching for a valid criterion for the adequacy of the relative pose between manipulator and object(s) to be handled, under the assumption that repositioning the robot is costly and that simultaneous repositioning and end-effector motion is not desired.

III. PROBLEM FORMULATION

In this section, we first state the problem of optimal coverage path planning ensuring least number of discontinuities. The problem is tailored to a polishing task with the introduction of additional task-specific constraints, as per the motivation of this work. These could be waived for a more generic exercise. Then, we show that the least number of discontinuities is independent of the choice of physical coverage path, so the original problem is transformed to an optimal cellular decomposition problem. Finally, the minimisation problem is further transformed to a colouring problem of the derived graph ensuring least number of different colours.

A. Problem Statement

Given the surface of an object, the manipulator kinematics and the shape and relative pose of obstacles in the workspace, under the assumption of a point contact between surface and EE, a valid coverage path consists of all valid joint-space poses of the manipulator that satisfy the following constraints:

- 1) Kinematic: the resulting manipulator motion is collision-free. When the EE contacts the surface, its z -axis is aligned with the normal vector of the surface at the contact point.
- 2) Force: when the EE contacts the surface, the manipulator is able to exert the required force along the z -axis.
- 3) Manipulability: when the EE contacts the surface, the manipulator should remain well-conditioned (under given manipulability measure [27]), to dispense with arising perturbations.

The optimal CPP problem is to find a valid joint-space path whereby the manipulator EE covers the workspace non-repetitively and ensures the least number of discontinuities.

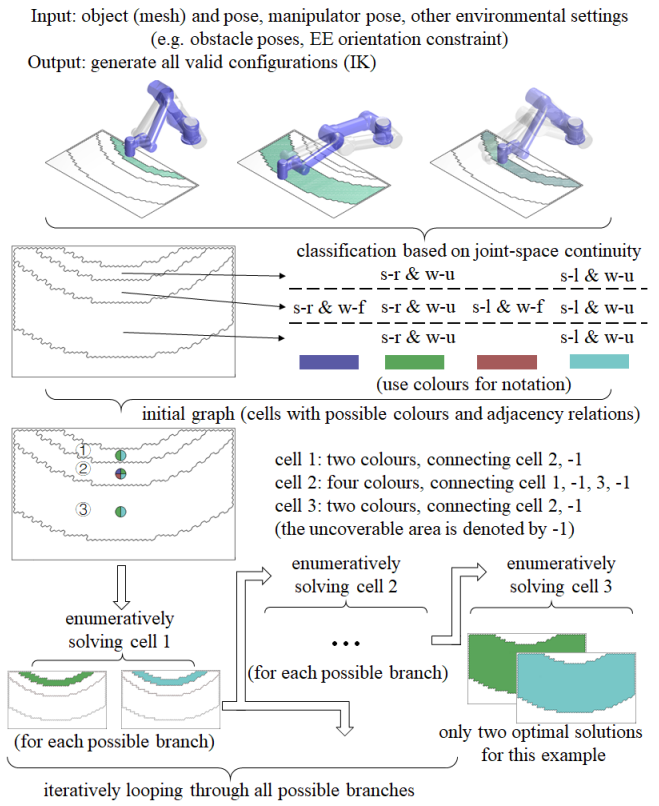


Fig. 3. Flow chart of the proposed coverage problem solver for optimal lift-off. The top section illustrates the different possible IK solutions to cover the same surface points. The vivid robot depiction shows the most common class of configuration: shoulder-right - (*s-r*) & (*w-u*) - wrist-unflipped, able to reach the three cyan areas on the flat surface. Configuration shoulder-left (*s-l*) & (*w-u*), shown shaded on the left-most figure can also reach the same areas. Two additional configurations (shown shaded on the right-most figure), (*s-r*) & (*w-f*) - wrist-flipped, and (*s-l* & *w-f*) are also valid, although they can only cover the middle part of the reachable area, in shaded cyan. An unpainted surface section indicates unreachable by any configuration. Each robot configuration is uniquely denoted, illustrated by a different colour. In collecting all valid configurations, since the manipulator is non-redundant, the space of valid configurations has the same 2-dimension as the task-space, and it is thus computable based on IK relations. A corresponding topological graph is generated based on the distribution of possible colours, and a solver is developed to reach all optimal solutions in proven finite steps. More details of the iterative solver process are provided in the text and in Fig. 4.

The optimal coverage process is illustrated on a flat surface problem by the flow chart shown in Fig. 3.

B. Independence from the Physical Coverage Path

An observation which simplifies the original problem is that manipulators are locally omni-directional in the joint-space, and configurations corresponding to a segment of coverage path without lift-off have high dimensional continuity in the joint-space, regardless of their sequencing order. As a result, this work is inspired to consider only continuous regions in the joint-space and its corresponding reachable area in the workspace, instead of coverage paths in the task space, which is equivalent to a cellular decomposition problem in the workspace considering joint-space continuity. Under this equivalence, complete visiting of each cell is guaranteed with any arbitrary joint-space continuous path within, without

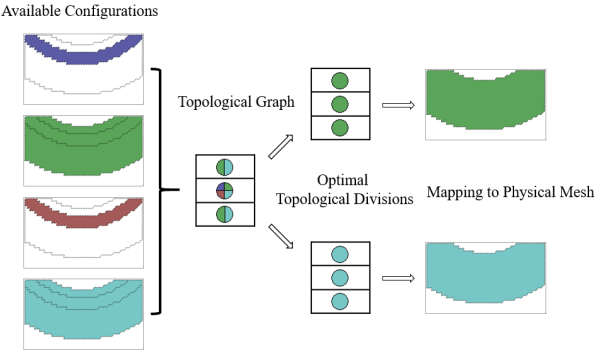


Fig. 4. Proposed cellular decomposition solver the set-up in Fig. 3. All configurations are divided into four disjoint (uniquely coloured) homogeneous sets, or cells, based on their joint-space continuities. The small circle filled-in with colour(s) represents all the possibilities to paint the corresponding area. A topological graph is created based on the distribution of the colours. Finally, in this example, two optimal options exist, both requiring zero lift-off.

discontinuities. Hence, once the cells are determined, the CPP problem within each cell is trivial, effectively transforming the design of the global coverage path in the traditional sense into a global cellular decomposition problem in joint-space, optimal in the number of lift-offs by incurring workspace partitions with minimum sets.

C. Modeling

Let \mathcal{C} be the set of all valid configurations and M be the set of all reachable points on the surface. The pose of the EE is also denoted by M since there is an one-to-one correspondence between the pose of the EE and the point on the surface, so we do not distinguish them.

Given a configuration $p \in \mathcal{C}$ covering $m \in M$, following the joint-space continuity, there exist a neighbourhood $(p \in) U_p \subset \mathcal{C}$ that can be reached continuously (without lift-off) from p , covering a section of surface $(m \in) V_m \subset M$. This is illustrated in Fig. 3, where the poses reached by the manipulator configuration depicted in vivid colour can be reached continuously - shown in vivid cyan. If any of them is chosen as p , then all of them are in U_p . Assuming there are some other unassigned configurations, i.e., $\mathcal{C} \setminus U_p \neq \emptyset$, choosing another $p' \in \mathcal{C} \setminus U_p$ specifies another set $V_{m'} \subset M$ - e.g. the shaded configurations depicted in Fig. 3. It is evident that $U_{p'} \cap U_p = \emptyset$. On repeating this process, all configurations are assigned a colour. Let the number of configurations be infinite. Actually, each valid configuration implies an open neighbourhood of valid configurations covering an open region on the surface (defined sub-resolutionally if the input data is discretized, like a triangular mesh in our case). The family of all open regions on the surface implied by all valid configurations is an infinite open cover of the whole surface which, with physical meaning, must have boundary. Then, even if there are infinite many open regions in the family, the Heine-Borel theorem in mathematical analysis claims the existence of a subcover with finite open regions. The finiteness of a discretised input data is trivial because the number of configurations is also finite. As such, \mathcal{C} is divided into a finite

number of disjoint sets, denoted by a finite number of different colours.

The problem also exploits the concept of a *cell* defined on the task-space, following the standard terminology of conventional cellular decomposition methods, but with the additional property of homogeneity. This is established on noticing that IK mapping from reachable points in the workspace to a single set of configurations is injective, since there is no non-singular path connecting two configurations whose EEs are at a same point (see graphic example in Fig. 1). The injectivity of each branch of the IK is the motivation to map the property of joint-space continuity back on to the surface, thus the algorithm can be visualized by drawing colours on the surface to form cells belonging to the same configuration class (colour). Referring to the same square coverage example, Fig. 4 shows how \mathcal{C} is divided into 4 disjoint sets. Since different IK solutions possess distinct colours, the available colours for points can be used to classify them. Let $\{c_i\}, i = 1, \dots, n$ be all the colours used, then for two points $m_1, m_2 \in M$ their sets of available colours are $c_{m_1} = \{c_{11}, \dots, c_{1i}\}, c_{m_2} = \{c_{21}, \dots, c_{2j}\}$. We then say that m_1 and m_2 belong to the same cell if and only if

$$\begin{cases} m_1, m_2 \text{ are connected} \\ \{c_{11}, \dots, c_{1i}\} = \{c_{21}, \dots, c_{2j}\} \end{cases}$$

Typically, for a triangular mesh surface as is our case, connectivity is provided by the edges of the mesh. Fig. 4 shows the creation of the cells.

Finally, a topological graph is created, whose elements are cells. Each cell possesses an index, records the possible colours and the indices of its adjacent cells in order, as per the example in Fig. 3. Since the number of colours is finite, the number of possible combinations of colours is also finite, which can be ordered as

$$\begin{cases} \{c_1\}, \dots, \{c_n\} \\ \{c_1, c_2\}, \dots, \{c_1, c_n\}, \{c_2, c_3\}, \dots, \{c_2, c_n\}, \dots, \{c_{n-1}, c_n\} \\ \dots \text{ (with all } i\text{-element combinations in the } i\text{-th row)} \\ \{c_1, \dots, c_n\} \end{cases}$$

For each combination of colours, the number of corresponding cells is finite, unless there are infinite many small cells with area zero, which is physically meaningless for the coverage task of the robots. In all, the number of cells must be finite.

After creating the topological graph, the cellular decomposition process is transformed into painting all points in a graph with one of their available colours. The number of solutions to “painting” the full graph means the number of coverage path segments, where discontinuities are required in between, with the minimum(s) as best solution. Two valid solutions exist for the example in Fig. 4. In summary, the proposed model of colouring a point in the surface to be covered means selecting a given IK solution for it, and the planning problem is thus transferred to designing a colour scheme for a topological configuration graph.

IV. ENUMERATIVE SOLVER FOR CELLULAR DECOMPOSITION

The difficulty of solving the coloring problem is that, although points are gathered into homogeneous cells, they can

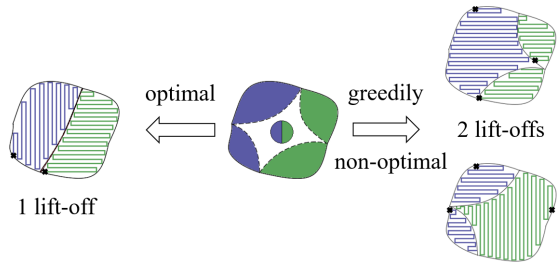
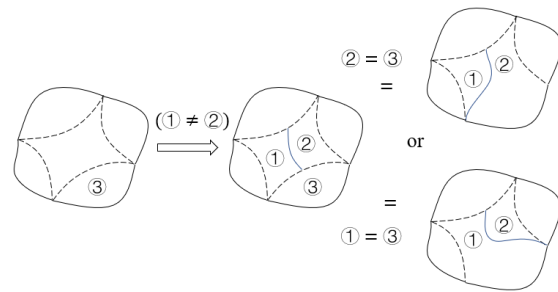
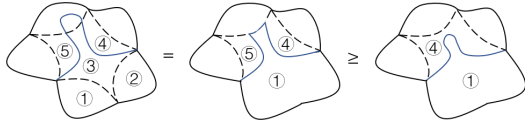


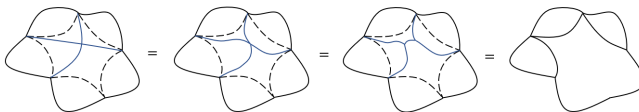
Fig. 5. In this example, only the middle cell still needs solving. From the two available colours, whatever the choice to fill the cell in its entirety incurs an extra, unnecessary lift-off. On the other hand, optimality is achieved when splitting the cell into two parts, with the two resulting sub-cells filled in with different colours, requiring only 1 lift-off.



(a) Example shows that it is sufficient to consider cutting path which starts and end at the topological edge endpoints.



(b) Example shows that it is unnecessary to consider cutting paths that stretch across edges.



(c) Example shows that intersecting cutting paths can be discarded.

Fig. 6. Unnecessary or sub-optimal cell divisions cases can be safely discarded.

be filled in with different colours, instead of only being seen as a whole and drawn with a single colour. The counter-example in Fig. 5 illustrates this phenomenon. By efficiently discarding equivalent cellular decompositions, it can be proven that the total number of different cellular decompositions is finite, thus all optimal solutions are finitely solvable.

A. Finiteness of Divisions

Since any path starting and ending at the boundary of a cell will divide the cell into two parts, there are infinite many physical solutions of dividing a cell into parts. However, there are only finite classes of them from a topological structure viewpoint because of the equivalence of physical divisions in the number of lift-offs.

Fig. 6(a) shows how cutting paths which start or end at a point other than an endpoint on an edge are unnecessary and can be pruned. Let a cutting path end at an arbitrary

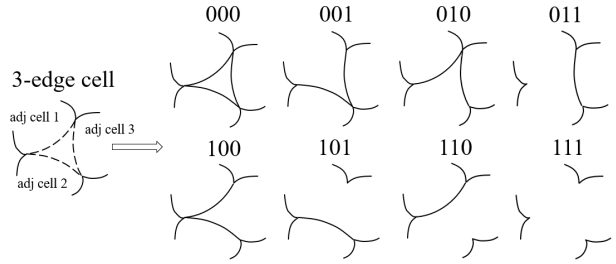


Fig. 7. Possible divisions of a 3-edge cell, as the most complex situation that need not further divisions. It can be observed how some of them are the same in terms of topological structure (e.g. 001, 010 and 100), or the division is impossible (e.g. 011 is enforced, but cell 1 and 2 do not have the same colour), it is clearly already a finite problem, and the description of further simplifications is omitted for clarity and space constraints.

point of the edge connecting with cell 3. From the definition of a cutting path, it implicitly enforces cell 1 and cell 2 having different colours. If $1 \neq 3$ and $2 \neq 3$ the division is trivial. However, for the depicted cases when $1 = 3$ or $2 = 3$, any cutting paths that start at any endpoint of the edge are equivalent. Hence, for a complete solution it is sufficient to only consider cutting paths which start and end at the endpoint of an edge.

Fig. 6(b) shows how cutting paths which go across any edge are unnecessary. Let a cutting path go across an edge, then cell 4 and cell 5 are prevented from being coloured together which leads to non-optimality, since they are separated physically by the cutting path.

Fig. 6(c) shows that cutting paths need not go across each other. When two cutting paths intersect, the resulting cutting path segments can be continuously transformed back onto the existing topological edges, and can be safely disregarded.

In conclusion, only cutting paths which start and end at the endpoint of topological edges and do not go across each other need to be considered when considering options for cell subdivision, making the total number of topological divisions finite.

B. Solution to Simple Cells

The following kinds of cells offer simple cases that can be solved directly without further divisions:

- 1) Cells containing less than four edges. They cannot be divided further into several cells with less number of topological edges. Fig. 7 enumerates all possible topological divisions for a three-edge cell, which constitutes the most complicated case for direct enumeration. Binary numbers are used to represent the edge connectivity, 1 (connected), 0 (disconnected). It is thus easy to see that there are at most 8 situations that require consideration.
- 2) Cells with only one possible colour.

C. Solution to Complex Cells

The concept of using binary coding for a simple cell is extended to solve for an arbitrary n -edge cell, with the addition of “ \times ” for a yet unspecified connectivity state that emanates from these more complex scenarios. For this binary

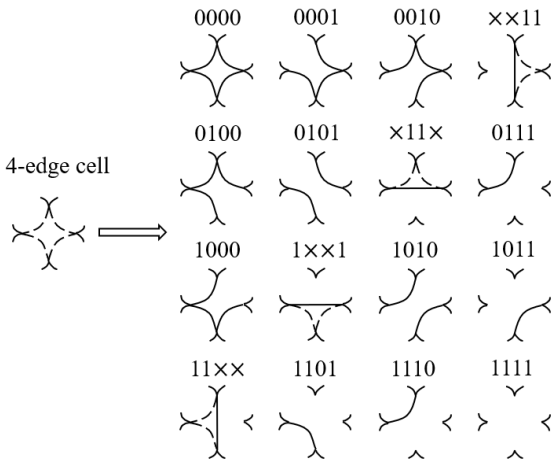


Fig. 8. The 2^4 possible divisions of an 4-edge cell. For the cell which has more than 3 edges, the sub-cell may be created. In this figure, the connectivities that correspond to generating a sub-cell is $\times \times 11$, $\times 11 \times$, $1 \times \times 1$, $11 \times \times$.

combination, there are less than $2^n \times m$ branches for an n -edge cell with m possible colours, so the problem remains finite. An example of solving for $n = 4$ is shown in Fig. 8. In this case, a continuous connected state (1s) implies that part of this cell must be painted with the same colour as that of the adjacent cells. On the other hand, a connectivity of 0 indicates that the topological edge between the cell and the corresponding adjacent cell is maintained, and as such the colours must be different.

The unspecified state \times indicates a sub-cell will be generated. A more detail discussion about the distinction between 0 and \times is warranted: when connectivity cases such as the following arise

$$1 \times \times 1, 1 \times \times \times 1, \dots$$

the cell is divided into smaller parts whose colours are enforced to be different, i.e. the cell needs further subdivision. Refer for instance to cases $\times \times 11$, $\times 11 \times$, $1 \times \times 1$, $11 \times \times$ in Fig. 8. The original cell transforms into a new one with fewer edges, since some (two for a 4-edge cell) edges are replaced by a single one. We use the bracket notation (\dots) in the binary number of the original cell to represent the generation of sub-cells. In recursively applying the same division for the applicable sub-cells, any n -edge cell can thus be continuously divided into a set of cells with fewer edges, suitable to then be solved enumeratively as described. Since sub-cells are generated from an original one, there are extra constraints on its connectivity as specified by the previous division. As such, the following situations may arise:

- 1) Single \times cannot form a sub-cell, because

$$\dots 1 \times 1 \dots = \dots 101 \dots \text{ or } \dots 111 \dots$$

but both conditions of the right side are considered in other branches. This is why the \times case does not apply to the 3-edge cell in Fig. 7.

- 2) The 0s can be freely moved outside the bracket, because of the equivalence

$$\dots \times 1(0 \times \dots \times 1)1 \times \dots = \dots \times 10(\times \dots \times 1)1 \times \dots$$

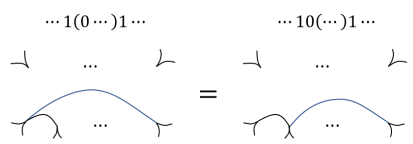


Fig. 9. The equivalence of moving the unconnected 0 state outside the bracket. Following this, in order to reduce the number of edges of a sub-cell, the equivalent sub-cell connectivity arrangement on the right is enforced.

See Fig. 9. The same is true for the right bracket based on the symmetry of the number list, since a cutting graph makes sense only when the inner two numbers at the boundary are 1s. This is why there are no brackets in Fig. 8.

- 3) The new topological edge created by a cutting path must be retained as it is manually introduced as such (it will always be 0, splitting a cell into different colours, it can not be 1 or \times). No extra possibilities appear after the division.

V. ITERATIVE SOLVER FOR CELLULAR DECOMPOSITION

With the enumerative solver as the basic building block, the graph can now be solved iteratively. Starting from a fully-unpainted graph, an unsolved cell is arbitrarily chosen and enumeratively solved as described in Section IV. Assuming a cell with n -edges with m possible colours, there are *at most* $2^n \times m$ possible divisions. A branch for each possible solution of the chosen cell is created, and in each branch the selected cell is filled in with the specified colour (so it will not change any more). In the next iteration, an unsolved branch is selected, and an unsolved cell within it, and repeat the same steps.

Note that the constraints given by the solved adjacent cells significantly restrict the possible solutions, because the state of an edge restricts the connectivity of the cells on both sides. Through iterative execution, if there is a cell who cannot satisfy all constraints given by its solved adjacent cells, then the graph cannot be painted using the current state of the even partly-filled painting scheme, orelse a valid coloring scheme for the graph can be generated which uniquely specifies the configuration to polish each equivalent workspace point amongst the various valid IK solutions it may exhibit.

The search algorithm runs on a deepest-first-searching (DFS) format, so that the memory requirements are reduced. As an exhaustive search protocol, all optimal physical cellular decompositions must be homeomorphic to one of the resulting schemes.

A. Cost Calculation

The physical meaning of the cost for a (partly filled) graph is the number of colour segments in the current portion of the graph, i.e. 1 colour equals cost = 1. The cost formulation is then described incrementally, whereby after a cell is solved

- 1) if its connectivity is all zero, then the cost will increase 1 after freshly coloring this cell.
- 2) if its connectivity has only one 1 connection to an already solved cell, then the cost will remain unchanged,

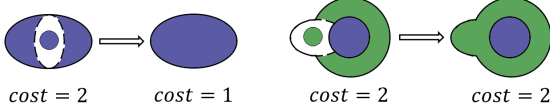


Fig. 10. Cost variation calculation. Left: the middle cell connects two distinct cells, so cost variation (1) is $1 - 2 = -1$. Right: two edges connect with the same adjacent cell, cost variation (1) is $1 - 1 = 0$.

TABLE I
UR5 MANIPULATOR KINEMATIC PARAMETERS

Joint i	α_i [rad]	a_i [m]	θ_i [rad]	d_i [m]
1	$\pi/2$	0	θ_1	0.089
2	0	-0.425	θ_2	0
3	0	-0.39225	θ_3	0
4	$\pi/2$	0	θ_4	0.11
5	$-\pi/2$	0	θ_5	0.09
EE	0	0	-	0.32

since the cell colour can be filled homogeneously with the connected adjacent cell.

- 3) if its connectivity has i 1s, there may exist multiple edges which connect the same adjacent cell, as per the illustration in Fig. 10. In order to be consistent with the physical meaning of the cost, if these edges connect j distinct solved cells, then the variation of cost is

$$\Delta\text{cost} = 1 - j \quad (1)$$

VI. EXPERIMENTAL RESULTS

The proposed algorithm performs non-repetitive coverage task using non-redundant manipulators of any dimension. Simulation and experimental examples emulating a polishing task on an object's surface are presented in this section implemented using a typical 6 DoF manipulator, a Universal Robots UR5. The kinematics of the 6 DoF manipulator are collected in Table I. For such endeavour, the (commonplace) final revolute joint of the manipulator is unnecessary given the rotating nature of the polishing tool itself. This is indeed the case for the UR5, and simulations and real evaluation have thus been undertaken where the last link has been locked.

In the first simulated experiment in Section VI-A a hemispherical object is polished at different poses in the workplace: one arbitrarily set, and the other precisely crafted to be fully reachable with the least number of lift-offs, which shows the ability of the proposed algorithm to also become a workspace design metric for evaluating the quality of the object placement to be inspected. The second simulated experiment in Section VI-B shows how the proposed algorithm can directly influence the choice of configurations to avoid non-optimal configurations that invariably lead to unnecessary lift-offs altogether. Additional examples with objects of arbitrary shape are collected in Section VI-C. Finally Section VI-D depicts real-world experiments with a UR5 manipulator polishing a wok in free space, and under the presence of obstacles, to prove the applicability of the proposed algorithm in real settings.

In the results shown hereafter the environment contains the manipulator, the object being polished, and where applicable

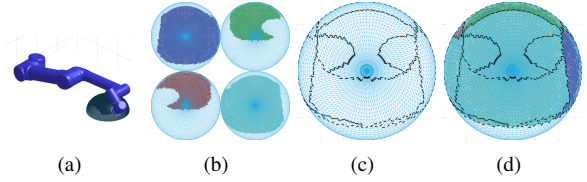


Fig. 11. (a) Hemispherical object arbitrarily placed in the workspace. (b) Coloured cells of four valid configuration, chosen by the optimal solution shown in (d). (c) Topological graph. (d) One optimal solution requiring 3 lift-offs (note how the manipulator cannot fully cover the farthest part of the mesh - the bottom area in the optimal solution, unpainted).

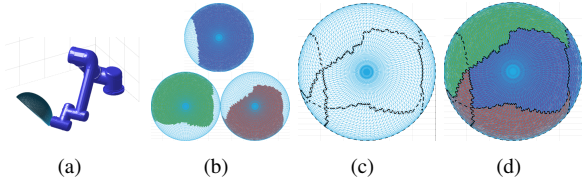


Fig. 12. (a) Hemispherical object placed obliquely in the workspace to achieve full coverage. (b) Coloured cells of three valid configuration, chosen by the optimal solution shown in (d). (c) Topological graph. (d) One optimal solution requiring only 2 lift-offs and achieving fully coverage, with the object fully painted over).

a ground plane and additional obstacles. Moreover, figures shown in this section are representative examples of arbitrary paths derived within the cells attained following the proposed optimal coverage solution.

A. Hemispherical Object (Object Placement Criterion)

A wok-like round mesh is used for this experiment. Results are collected in Fig. 11 and Fig. 12. In the former, the object is arbitrarily placed with respect to the robot, as would be the case, for instance, on an automated production line with unsorted objects are fed via a conveyor belt. A CPP is designed following the proposed scheme. With no criterion for the placement, the algorithm shows that such an object placement requires at least 3 lift-offs to inspect the reachable area, yet fails in attaining full coverage (the farthest area, shown at the bottom of the mesh, is out-of-bounds). Fig. 12 illustrates the case where the proposed coverage strategy reveals a suitable pose for the object so that not only the required least number of lift-offs is decreased to 2 when compared to the arbitrary placement, but the manipulator can fully cover the surface.

B. Cylindrical Object (Pruning of Suboptimal Configurations)

Polishing of a half-pipe is employed in this simulation to demonstrate how the proposed algorithm can identify and bypass unnecessary configurations leading to “traps” that cause CPPs with extra lift-offs.

The pipe is placed obliquely to achieve full coverage. Surface normals vary along the arc length of the cylinder over π radians, which cause increased difficulty in kinematic terms for the manipulator to sustain the desired polishing operation. The topological graph and optimal solution are shown in Fig. 13, where it can be seen that the full coverage task requires only 1 lift-off. However, there are many valid configurations which lead to non-optimality. See Fig. 14 for

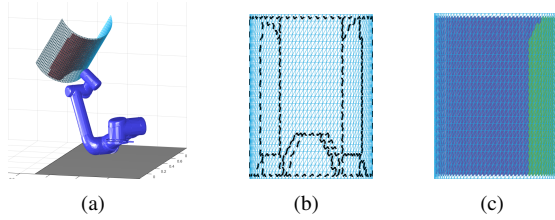


Fig. 13. (a) A cylindrical half-pipe object. (b) The topological graph. (c) One optimal solution which requires only 1 lift-off.

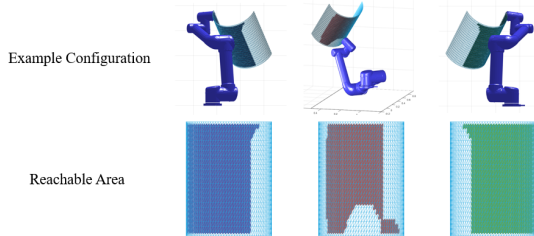


Fig. 14. Example with three different configurations and their reachable area. Once any configuration belonging to the middle cell is chosen to cover the surface, sooner or later it will have to change to the left and right cells to finish the full coverage of the surface, thus incurring a wasteful lift-off.

an example of such “trap” configurations. The configurations on the left and right are the ones finally chosen by one of the optimal solutions shown in Fig. 13. However, while the configuration in the middle can cover a large area without lift-offs, and would therefore be equally likely to be chosen if the IK solutions were to be selected randomly or in a greedy fashion, it cannot reach the corners of the mesh (eventually covered by the other two configurations). Hence, should any configuration from the middle be selected to trace the object, after coverage of (a section) of the middle part of the pipe, sooner or later the CPP will have to undertake one unnecessary lift-off for full coverage inspection, leading to non-optimality when compared to the case shown in Fig. 13. The proposed algorithm will provide all optimal solutions, with none of them using the middle coloured cell.

C. Arbitrary Shape Objects and Comparative Analysis

Further simulation tests are also shown on Fig. 15 and 16, where the robot arm was made to fully trace the surface of objects of arbitrary shape with the proposed algorithm. In the former instance a vase is considered, whereas a full-pipe is consider in the latter.

To better appreciate the effectiveness of the proposed scheme, a comparative analysis is provided to contrast key relevant metrics with a standard geometric planner. Number of lift-offs and total time taken to complete the coverage task were collected and are shown in Table II. For a fair evaluation, the pure spiral and boustrophedon planners are assumed to know in advance the non-reachable points on the surface, so they can be disregarded. Given the reliance of these planners on the starting point of the paths, the results are averaged over 10 runs where random starting points are observed. A variety of objects are studied, beyond those singled out in the previous sections - individual detailed solutions for each case are omitted

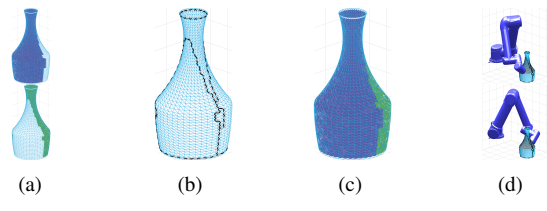


Fig. 15. Vase example. (a) Reachable coloured cells of two valid configurations, chosen by the optimal solution shown in (c). (b) Topological graph. (c) One of the optimal solutions requiring only 1 lift-off. The cutting path is arbitrary. (d) Examples of poses in the two types of configurations.

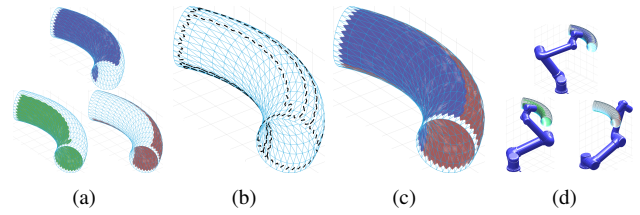


Fig. 16. Full-pipe example. (a) Reachable coloured cells of two valid configurations, chosen by the optimal solution shown in (c). (b) Topological graph. (c) One of the optimal solutions requiring only 1 lift-off. The cutting path is arbitrary. (d) Examples of poses in the four types of configurations.

given space limitations. It is clearly apparent how the optimal solution suggested by the proposed CPP planner markedly outperforms any of the other planners for the coverage task.

D. Real World Experiments in the Presence of Obstacles

A Universal Robots UR5 manipulator is employed for real experimentation to polish the outer surface of a wok to show a physical coverage path generated based on the proposed cellular decomposition method. The actual physical coverage path uses a simple back-and-forth motion (boustrophedon) within the resulting cells, with a lift-off concatenation between paths segments belonging to different cells. The reader is referred to the associated video¹ for the full demonstration. As discussed, the manipulator operates in a 5 DoF configuration. Since hybrid position/force control [15] is beyond the scope of this work, contact is restricted to position control.

Fig. 17 illustrates the results. Given the location of the wok, it can be seen how the nearest part of the wok is unreachable. As can be observed in Fig. 17(d) and 17(e), the manipulator must keep its wrist configured in the “above” the fore-arm configuration in order to avoid collisions, which leads to the two shoulder-left and shoulder-right configuration solutions. The total number of lift-offs is 1. Note that any division keeping the resulting cell connectivity guarantees full (reachable) coverage and is optimal in the minimum number of lift-offs, so the cutting path dividing the final cell is arbitrary.

A more interesting example arises when the motion of the manipulator is obstructed by the cylindrical obstacle depicted in Fig. 18. Since the obstacle may collide with the upper-arm, fore-arm or the EE, and the wrist may collide with the fore-arm, the resulting colour cell decomposition and the topological graphs is more complex. As such, to avoid collisions, the least number of lift-offs is shown to be 2.

TABLE II
COVERAGE PLANNERS COMPARISON

	Ours(with Boust.)		Pure Spiral (10 average)		Pure Boust. (10 average)	
	Lift-offs	Time	Lift-offs	Time	Lift-offs	Time
Hemisphere	2	3175.9	35.6	1503.3	3.5	3941.3
Half pipe	1	840.75	33.2	1055.8	3.3	768.4
Vase	1	1101.47	31.4	2425.2	2.8	902.76
Full pipe	3	924.47	86.4	3365	59.8	3608.8

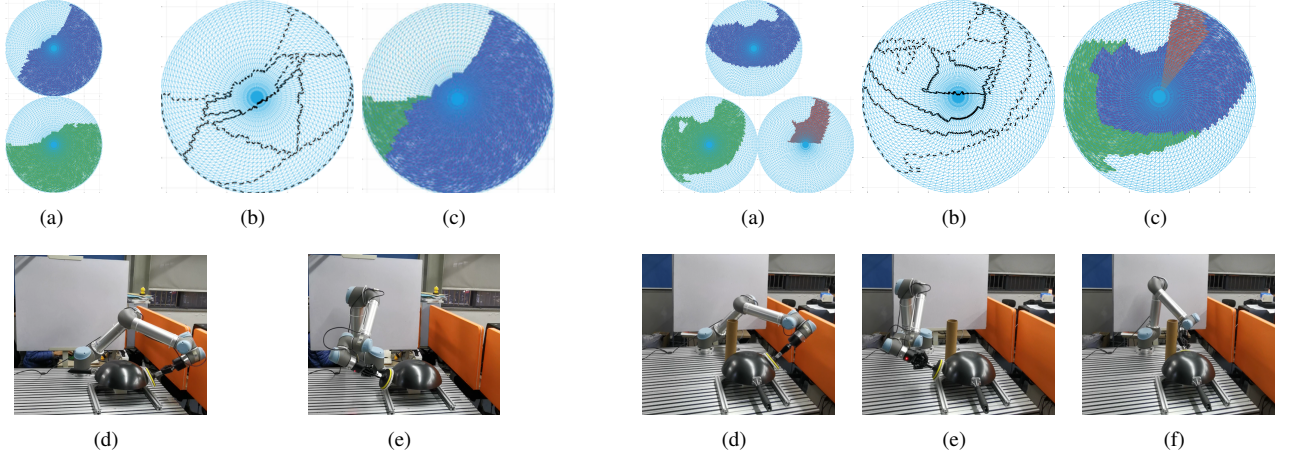


Fig. 17. (a) Reachable coloured cells of two valid configurations, chosen by the optimal solution shown in (c). (b) Topological graph. (c) One of the optimal solutions requiring only 1 lift-off. The cutting path is arbitrary. (d),(e) Examples of extreme poses in the two types of configurations.

VII. CONCLUSION

A novel proposition for the coverage planning problem has been developed in this work. The key metric is the minimum number of coverage path discontinuities, predicated on the need for tasks such as polishing, painting or deburring to curtail the number of robot lift-offs for proficient results, most prominently within the context of its application in automated industrial settings and increase productivity.

To this end, instead of considering the design of a coverage path in the traditional sense, this research considers the global optimal cellular decomposition problem in joint-space to assemble minimum sets that guarantee homogeneous joint-space configurations. In noting that IK mapping from the reachable points in the workspace to a single set of configurations is injective, colouring a point in the surface to be covered means selecting a given IK solution for it, and the planning problem is transferred to designing a colour scheme for a topological configuration graph. The proposed scheme thus provides two relevant contributions to the CPP problem in relation to optimal discontinuities: (a) proof that the least number of discontinuities, or “lift-offs”, is independent of the choice of coverage path, and (b) suggesting a novel cellular decomposition strategy to efficiently discard of equivalent cells. In proving that the total number of different cellular decompositions is finite, all optimal solutions are demonstrated finitely solvable.

After applying any conventional CPP algorithm in each resulting cell, the nominated algorithm thus generates a coverage path containing the least number of discontinuities. As a direct

Fig. 18. (a) Reachable coloured cells of three valid configuration, chosen by the solution in (c). (b) Topological graph. (c) One of the optimal solutions, requiring 2 lift-offs. (d),(e),(f) Example of the three kinds of configurations, where (d) Example of the shoulder-left configuration adopted to avoid collision between the upper-arm and the obstacle. (e) Example of the wrist above the fore-arm configuration, so that the wrist avoids colliding with the fore-arm. (f) An example of the only valid configuration to cover the points in the brown cell, situating the wrist below the fore-arm.

corollary, the scheme can be applied to any other cellular decomposition methods in the literature (e.g. Morse-based), to produce the least number of discontinuities obeying the given cellular decomposition method. It can also be exploited as a criterion to evaluate placement of a manipulator or object in the workspace for minimal lift-off coverage paths. A systematic methodology to resolve this topic is left for future work. Extensive simulation and a real-world implementation on a 5 DoF manipulator in realistic conditions are presented, supplemented by a detailed video. A comprehensive comparison with other geometric CPPs show the merit of the scheme and proves the validity of the proposed strategy in producing highly effective coverage paths.

ACKNOWLEDGMENT

This work was supported in part by the National Key Research and Development Program of China under Grant 2018YFB1309300 and in part by the National Nature Science Foundation of China under Grant U1609210 and Grant 61903332.

REFERENCES

- [1] J. Molina, J. E. Solanes, L. Arnal, and J. Tornero, “On the detection of defects on specular car body surfaces,” *Robotics and Computer-Integrated Manufacturing*, vol. 48, pp. 263–278, 2017.

- [2] M. Li, Z. Lu, C. Sha, and L. Huang, "Trajectory generation of spray painting robot using point cloud slicing," *Applied Mechanics and Materials*, vol. 44–47, pp. 1290–1294, 2011.
- [3] X. Xie and L. Sun, "Force control based robotic grinding system and application," in *2016 12th World Congress on Intelligent Control and Automation (WCICA)*, pp. 2552–2555, 2016.
- [4] F. Tian, Z. Li, C. Lv, and G. Liu, "Polishing pressure investigations of robot automatic polishing on curved surfaces," *The Int. J. of Advanced Manufacturing Technology*, vol. 87, no. 1, pp. 639–646, 2016.
- [5] H. Choset, "Coverage for robotics – a survey of recent results," *Annals of Mathematics and Artificial Intelligence*, vol. 31, no. 1, pp. 113–126, 2001.
- [6] E. Galceran and M. Carreras, "A survey on coverage path planning for robotics," *Robotics and Autonomous Systems*, vol. 61, no. 12, pp. 1258–1276, 2013.
- [7] Z. Xie, L. Jin, X. Du, X. Xiao, H. Li, and S. Li, "On generalized rmp scheme for redundant robot manipulators aided with dynamic neural networks and nonconvex bound constraints," *IEEE Transactions on Industrial Informatics*, vol. 15, pp. 5172–5181, Sep. 2019.
- [8] Z. Xie, L. Jin, X. Luo, S. Li, and X. Xiao, "A data-driven cyclic-motion generation scheme for kinematic control of redundant manipulators," *IEEE Transactions on Control Systems Technology*, pp. 1–11, 2020.
- [9] G. Oriolo and C. Mongillo, "Motion planning for mobile manipulators along given end-effector paths," in *Robotics and Automation, 2005. ICRA 2005. Proceedings of the 2005 IEEE International Conference on*, 2005.
- [10] J. Porta and L. Jaillet, "Path planning on manifolds using randomized higher-dimensional continuation," vol. 68, pp. 337–353, 01 2010.
- [11] J. M. Porta, L. Jaillet, and O. Bohigas, "Randomized path planning on manifolds based on higher-dimensional continuation," *International Journal of Robotics Research*, vol. 31, no. 2, pp. 201–215, 2012.
- [12] M. Hassan and D. Liu, "A deformable spiral based algorithm to smooth coverage path planning for marine growth removal," pp. 1913–1918, 2018.
- [13] S. S. S. Mirrazavi and B. Aude, "A dynamical-system-based approach for controlling robotic manipulators during noncontact/contact transitions," *IEEE Robotics & Automation Letters*, vol. 3, no. 4, pp. 2738–2745, 2018.
- [14] J. E. Solanes, L. Gracia, P. Munozbenavent, A. Esparza, J. Valls Miro, and J. Tornero, "Adaptive robust control and admittance control for contact-driven robotic surface conditioning," *Robotics and Computer-integrated Manufacturing*, vol. 54, pp. 115–132, 2018.
- [15] J. E. Solanes, L. Gracia, P. Munozbenavent, J. Valls Miro, C. Perezval, and J. Tornero, "Robust hybrid position-force control for robotic surface polishing," *Journal of Manufacturing Science and Engineering-transactions of The Asme*, vol. 141, no. 1, p. 011013, 2019.
- [16] V. J. Lumelsky, S. Mukhopadhyay, and K. Sun, "Dynamic path planning in sensor-based terrain acquisition," *IEEE Transactions on Robotics and Automation*, vol. 6, no. 4, pp. 462–472, 1990.
- [17] H. Choset, E. U. Acar, A. A. Rizzi, and J. Luntz, "Exact cellular decompositions in terms of critical points of morse functions," vol. 3, pp. 2270–2277, 2000.
- [18] E. U. Acar, H. Choset, A. A. Rizzi, P. N. Atkar, and D. Hull, "Morse decompositions for coverage tasks," *The International Journal of Robotics Research*, vol. 21, no. 4, pp. 331–344, 2002.
- [19] H. Choset, K. M. Lynch, S. Hutchinson, G. Kantor, W. Burgard, L. Kavraki, and S. Thrun, *Principles of Robot Motion: Theory, Algorithms, and Implementation*. MIT Press, 2005.
- [20] H. Choset and P. Pignon, "Coverage path planning: The boustrophedon cellular decomposition," pp. 203–209, 1998.
- [21] H. Choset, "Coverage of known spaces: The boustrophedon cellular decomposition," *Autonomous Robots*, vol. 9, no. 3, pp. 247–253, 2000.
- [22] H. Choset and J. W. Burdick, "Sensor-based exploration: The hierarchical generalized voronoi graph," *The International Journal of Robotics Research*, vol. 19, no. 2, pp. 96–125, 2000.
- [23] P. Atkar, H. Choset, and A. Rizzi, "Towards optimal coverage of 2-dimensional surfaces embedded in \mathbb{R}^3 : choice of start curve," in *Proceedings of 2003 IEEE/RSJ International Conference on Intelligent Robots and Systems (IROS '03)*, vol. 4, pp. 3581 – 3587, October 2003.
- [24] W. H. Huang, "Optimal line-sweep-based decompositions for coverage algorithms," in *Proceedings 2001 ICRA. IEEE International Conference on Robotics and Automation (Cat. No.01CH37164)*, vol. 1, pp. 27–32 vol.1, May 2001.
- [25] P. A. Jimenez, B. Shirinzadeh, A. E. Nicholson, and G. Alici, "Optimal area covering using genetic algorithms," *international conference on advanced intelligent mechatronics*, pp. 1–5, 2007.
- [26] F. Paus, P. Kaiser, N. Vahrenkamp, and T. Asfour, "A combined approach for robot placement and coverage path planning for mobile manipulation," in *2017 IEEE/RSJ International Conference on Intelligent Robots and Systems (IROS)*, 2017.
- [27] T. Yoshikawa, "Translational and rotational manipulability of robotic manipulators," *American Control Conference*, vol. 27, pp. 228–233, 1990.



Tong Yang is currently pursuing the Ph.D. degree with the Institute of Cyber-Systems and Control, Department of Control Science and Engineering, Zhejiang University, Hangzhou, China. His current research interests include robot planning and control.



Jaime Valls Miro received his B.Eng. and M.Eng. in Computer Systems from the Valencia Polytechnic University (UPV, Spain). He received his Ph.D. in robotics and control systems from Middlesex University (UK). He is currently an Associate Professor at the Centre for Autonomous Systems in UTS (Australia). His areas of interest span across the field of robotics, most notably modelling sensor behaviours for perception and mapping, computational Intelligence in HRI , and robot navigation.



Qianan Lai is currently pursuing the master degree with the Institute of Cyber-Systems and Control, Department of Control Science and Engineering, Zhejiang University, Hangzhou, China. His current research interests include robot grasping and robotics vision.



Yue Wang is currently a Post-Doctotral Fellow with the Institute of Cyber-Systems and Control, Department of Control Science and Engineering, Zhejiang University, Hangzhou, China. His current research interests include mobile robotics and robot perception.



Rong Xiong is currently a Professor with the Institute of Cyber-Systems and Control, Department of Control Science and Engineering, Zhejiang University, Hangzhou, China. Her current research interests include robot planning and robotics vision.